

See discussions, stats, and author profiles for this publication at: <https://www.researchgate.net/publication/254991505>

# Mechanistic studies of copper thin-film growth from CuI and CuII $\beta$ -diketonates

ARTICLE *in* JOURNAL OF THE AMERICAN CHEMICAL SOCIETY · FEBRUARY 1993

Impact Factor: 12.11 · DOI: 10.1021/ja00056a028

---

CITATIONS

131

---

READS

23

3 AUTHORS, INCLUDING:



Lawrence Dubois

ATMI Materials Ltd.

105 PUBLICATIONS 6,730 CITATIONS

SEE PROFILE

# Mechanistic Studies of Copper Thin-Film Growth from Cu<sup>I</sup> and Cu<sup>II</sup> $\beta$ -Diketonates

Gregory S. Girolami,<sup>\*,†</sup> Patrick M. Jeffries,<sup>†</sup> and Lawrence H. Dubois<sup>\*,‡</sup>

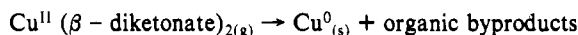
Contribution from the School of Chemical Sciences, The University of Illinois, Urbana, Illinois 61801, and AT&T Bell Laboratories, Murray Hill, New Jersey 07974.  
Received July 20, 1992

**Abstract:** The kinetics and mechanism of copper film growth from the reactions of bis(acetylacetonato)copper(II), bis(hexafluoroacetylacetonato)copper(II), and (vinyltrimethylsilane)(hexafluoroacetylacetonato)copper(I) (Cu(hfac)(vtms)) with copper single crystal surfaces were investigated. Experiments were performed using vibrational spectroscopy (reflection infrared and high-resolution electron energy loss spectroscopies) as well as mass spectrometry (temperature-programmed desorption and integrated desorption mass spectrometry). Both ligand desorption and dissociation were observed upon pyrolysis of these molecules under ultra-high-vacuum conditions. We demonstrate that adsorbed  $\beta$ -diketonate ligands decompose in a stepwise fashion at temperatures above  $\sim 375$  K to yield adsorbed CF<sub>3</sub> and ketylidene ( $\equiv\text{C}-\text{C}\equiv\text{O}$ ) intermediates. These further decompose above  $\sim 500$  K to leave surface carbon, a major contaminant in copper films grown from Cu<sup>II</sup>  $\beta$ -diketonates. Clean films can be grown from the pyrolysis of Cu(hfac)(vtms) at pressures above  $10^{-5}$  Torr, however. The implications of our results relative to the mechanism of copper film growth at elevated pressures are also discussed.

## 1. Introduction

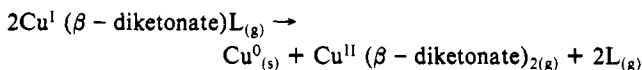
As feature sizes in integrated circuits shrink to  $0.25\ \mu\text{m}$  and below, both the conductivity and the electromigration resistance of the contact material become increasingly important. Copper is thus a reasonable alternative to more commonly used materials such as tungsten and aluminum-silicon alloys. The conductivity of copper is 5 times that of tungsten, while the electromigration resistance is almost 4 orders of magnitude better than that of pure aluminum.<sup>1,2</sup> In addition, due to the design specifications of the substrate architecture (where high aspect ratio ( $>3:1$ ) vias and plugs must be filled), film growth by chemical vapor deposition (CVD) may be required.

Several classes of CVD precursors have proven useful for the deposition of copper thin films.<sup>3-10</sup> Two of the most promising are copper(II)  $\beta$ -diketonates<sup>3,4</sup> and Lewis base adducts of copper(I)  $\beta$ -diketonates.<sup>5,6</sup> Although structurally similar, these complexes behave quite differently under CVD conditions. Copper(II)  $\beta$ -diketonates generate copper films that are often contaminated by carbon; presumably the incorporation of carbon contaminants is due to fragmentation of the  $\beta$ -diketonate ligands.<sup>11,12</sup>



It has been reported, however, that clean copper films can be deposited in a very narrow temperature range from pure bis(hexafluoroacetylacetonato)copper(II) (Cu(hfac)<sub>2</sub>).<sup>4</sup> More typically, depositions are conducted using a carrier gas such as hydrogen, which acts as a reducing agent and aids in the removal of the  $\beta$ -diketonate ligands and their decomposition products from the growing copper film.<sup>3,4,13</sup>

In contrast, copper(I)  $\beta$ -diketonate complexes can yield pure copper films under a variety of conditions, even in the absence of hydrogen, because the deposition occurs via the surface disproportionation reaction<sup>5,6</sup>



where L is a typical Lewis base. If this reaction takes place at a temperature lower than that at which either Cu<sup>II</sup> ( $\beta$ -diketonate)<sub>2</sub> or L decompose, then the products desorb intact from the surface and the resulting copper film is free of carbon impurities.

We have begun a program to elucidate both the kinetics and mechanism of copper film growth from CVD precursors, and here we describe studies of a representative of each of these two

classes:<sup>12</sup> Cu(hfac)<sub>2</sub> and (vinyltrimethylsilane)(hexafluoroacetylacetonato)copper(I) (Cu(hfac)(vtms)). Both of these materials are stable, have relatively high vapor pressures,<sup>4,6</sup> and have been shown to deposit pure copper films at low temperatures. The chemistry of these molecules has been studied on Cu(111) and Cu(100) single crystal substrates in ultra-high-vacuum (UHV) in order to model the types of surface processes that may take place under steady-state growth conditions. Several questions are addressed in our work: (1) What are the surface species present at different temperatures? (2) What are the activation energies for the various reactions that take place during film growth? (3) What is the minimum temperature at which the disproportionation of Cu(hfac)(vtms) can occur? (4) What is the chemical mechanism by which hfac ligands fragment? and (5) What is the source of carbon within the hfac ligand that becomes incorporated into the growing copper film?

Perhaps the most interesting result of our investigations is the observation that ketylidene groups ( $\equiv\text{C}-\text{C}\equiv\text{O}$ ) are formed upon fragmentation of hfac ligands. These intermediates decarbonylate above 500 K to generate surface carbon atoms that can become incorporated as undesirable contaminants in copper films grown from pure Cu(hfac)<sub>2</sub>. Comparative studies of the surface chemistry of the unfluorinated precursor bis(acetylacetonato)copper(II) (Cu(acac)<sub>2</sub>)<sup>14</sup> as well as those of the organic

- (1) Shingubara, S.; Nakasaki, Y.; Kaneko, H. *Appl. Phys. Lett.* **1991**, *58*, 42.
- (2) Kang, H. K.; Choe, J.; Asano, I.; Wong, S. *Proc. VMIC Conf.* June, 1992, in press.
- (3) Van Hemert, R. L.; Spendlove, L. B.; Sievers, R. E. *J. Electrochem. Soc.* **1965**, *112*, 1123.
- (4) Temple, D.; Reisman, A. *J. Electrochem. Soc.* **1989**, *136*, 3525.
- (5) Shin, H.-K.; Chi, K. M.; Hampden-Smith, M. J.; Kodas, T. T.; Farr, J. D.; Paffett, M. F. *Adv. Mater.* **1991**, *3*, 246; *Mat. Res. Soc. Symp. Proc.* **1991**, *204*, 421; *Chem. Mater.* **1992**, *4*, 788.
- (6) Norman, J. A. T.; Muratore, B. A.; Dyer, P. N.; Roberts, D. A.; Hochberg, A. K. *J. Phys. IV* **1991**, *1*, C2-263.
- (7) Jeffries, P. M.; Girolami, G. S. *Chem. Mater.* **1989**, *1*, 8. Jeffries, P. M.; Dubois, L. H.; Girolami, G. S. *Chem. Mater.* **1992**, *4*, 1169.
- (8) Gross, M. E. *J. Electrochem. Soc.* **1991**, *138*, 2422.
- (9) Beach, D. B.; LeGoues, F. K.; Hu, C.-K. *Chem. Mater.* **1990**, *2*, 216.
- (10) Beach, D. B.; Kane, W. F.; LeGoues, F. K.; Knors, C. J. *Mater. Res. Soc. Symp. Proc.* **1990**, *181*, 73.
- (11) Hampden-Smith, M. J.; Kodas, T. T.; Paffett, M.; Farr, J. D.; Shin, H.-K. *Chem. Mater.* **1990**, *2*, 636.
- (12) Gross, M. E.; Donnelly, V. M. In *Proc. Adv. Metal. ULSI Appl.* Rana, V. V. S.; Joshi, R. V.; Ohdomari, I., Eds. **1992**, 355. Donnelly, V. M.; Gross, M. E. *J. Vac. Sci. Technol.* In press.
- (13) Dubois, L. H.; Jeffries, P. M.; Girolami, G. S. In *Proc. Adv. Metal. ULSI Appl.* Rana, V. V. S.; Joshi, R. V.; Ohdomari, I., Eds. **1992**, 375.
- (14) Kaloyeros, A. E.; Feng, A.; Garhart, J.; Brooks, K.; Ghosh, S.; Saxena, A.; Lehrs, F. *J. Electron. Mat.* **1990**, *19*, 271.
- (15) Films grown from Cu(acac)<sub>2</sub> are very similar to those grown from Cu(hfac)<sub>2</sub>: Pauleau, Y.; Fasasi, A. Y. *Chem. Mater.* **1991**, *3*, 45.

<sup>†</sup> The University of Illinois.

<sup>‡</sup> AT&T Bell Laboratories.

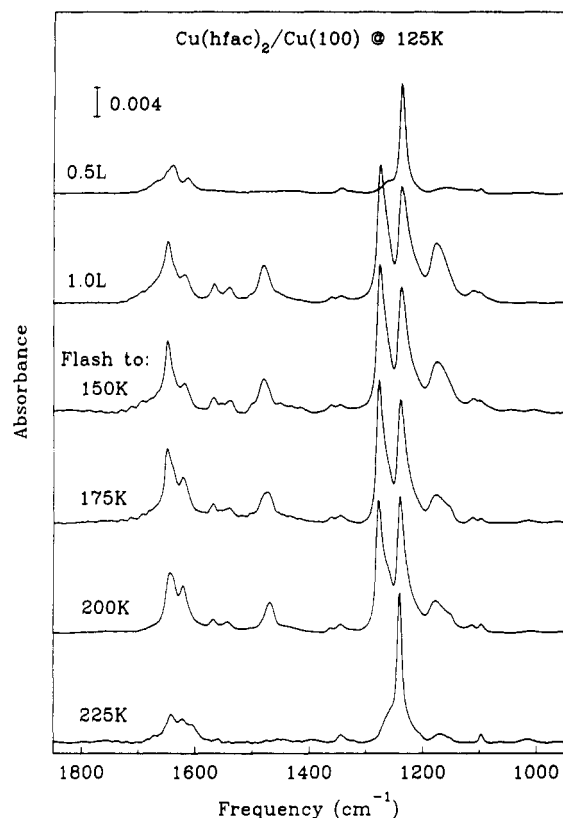


**Figure 1.** Infrared spectrum of a Cu(100) surface exposed to 0.5 L of Cu(hfac)<sub>2</sub> at 125 K (upper trace). As the gas exposure is increased to 1.0 L, a multilayer of Cu(hfac)<sub>2</sub> is formed. The mode assignments are summarized in Table I. The vibrational spectrum is similar to that of gas-phase or crystalline Cu(hfac)<sub>2</sub>.<sup>12,17-19</sup> As the temperature is raised above ~200 K, the multilayer desorbs and the vibrational spectrum of surface bound hfac ligands is observed (see text). All spectra were recorded at 125 K.

ligands hexafluoroacetylacetone (hfacH), acetylacetone (acacH), and vinyltrimethylsilane (vtms) have also been carried out.

## 2. Results and Discussion

**Low-Temperature Adsorption Studies.** The top trace of Figure 1 shows a reflection-absorption infrared (RAIR) spectrum of a clean Cu(100) surface exposed to 0.5 L of Cu(hfac)<sub>2</sub> at 125 K. The spectrum is dominated by a single C–F stretching vibration at 1239 cm<sup>−1</sup>; we will show presently that this feature is due to adsorbed hfac ligands oriented perpendicular to the surface plane. This observation of a ligand dissociation process at low temperatures is consistent with recent X-ray photoelectron spectroscopy (XPS) studies of Pd(hfac)<sub>2</sub> and Cu(hfac)<sub>2</sub> adsorption on polycrystalline copper foils which also show that at low gas doses (≤1 L) the hfac ligands migrate away from the central metal atom to the surface, even at 120 K.<sup>15</sup> We note that this ligand migration process is much faster on a metal surface than it is in solution, where the activation energy for hfac/hfacH exchange in Cu(hfac)(diphenylacetylene) is 14.4 kcal/mol.<sup>16</sup>

The addition of another 0.5-L dose of Cu(hfac)<sub>2</sub> to the copper surface at 125 K (1.0 L total gas exposure) changes the infrared spectrum dramatically. The new spectrum is almost identical to that of crystalline Cu(hfac)<sub>2</sub><sup>17-19</sup> and implies that a multilayer of randomly oriented precursor is present on the surface at 125 K. A similar spectrum is observed for a 50-L gas exposure. Mode assignments for the multilayer are summarized in Table I. The

**Table I.** Observed Vibrational Frequencies and Mode Assignments for Cu(hfac)<sub>2</sub><sup>a</sup>

Cu(100), 125 K <sup>b</sup>	KBr <sup>c</sup>	Cu(100), 300 K <sup>d</sup>	Cu(111), 300 K <sup>e</sup>	assignment <sup>f</sup>
	3084		3090	CH stretch
			2825	1220 + 1605
			2635	1220 + 1405
			2445	2 × CF <sub>3</sub> stretch
			2285	1220 + 1065
1648	1648	~1625		C=C stretch
1619	1619	1607	1605	C=O stretch
1567	1565			CO stretch +
1540	1538			CH bend
1482	1470		1405	CC stretch +
1360, 1341	1357	1332		CCF <sub>3</sub> stretch
1275, 1238	1256, 1208	1238	1220	CF <sub>3</sub> stretch <sup>g</sup>
1176	1148	1147		CH bend
1097	1105	1093	1065	CH bend
	808		790	C–CF <sub>3</sub> stretch,
	749		725	bend
	683, 600		645	ring deformation
	531		575, 445	Cu–O stretch

<sup>a</sup> All frequencies in cm<sup>−1</sup>. <sup>b</sup> IR, Figure 1. <sup>c</sup> Reference 19. <sup>d</sup> IR, Figure 11. <sup>e</sup> EELS, Figure 6a. <sup>f</sup> References 17 and 18. <sup>g</sup> By analogy with the normal coordinate analysis for Cu(acac)<sub>2</sub><sup>20</sup> and for substituted trifluoromethanes,<sup>21</sup> we assign the higher frequency band to the asymmetric stretch and the lower frequency band to the symmetric CF<sub>3</sub> stretch.

spectrum contains strong peaks due to the hfac ligand, including intense C–F stretching modes at 1265 and 1221 cm<sup>−1</sup>, a C–C stretching band at 1648 cm<sup>−1</sup>, a C–H in-plane bend at 1176 cm<sup>−1</sup>, and various weaker features due to C=O stretching modes, C–H, C–C, and C–O bending modes, and overtone and combination bands. The spectrum remains essentially unchanged (other than small intensity variations) at substrate temperatures up to 200 K (Figure 1, middle traces).

Between 200 and 225 K, the spectrum again changes dramatically (Figure 1, bottom trace) and no longer resembles that of pure Cu(hfac)<sub>2</sub>. The spectrum is now almost identical to that of a clean copper surface dosed with 0.5 L of Cu(hfac)<sub>2</sub> at 125 K (Figure 1, upper trace). Clearly the multilayer has desorbed by 225 K, once again leaving a monolayer of hfac ligands. This observation is consistent with recent XPS data on the adsorption of Cu(hfac)<sub>2</sub> on polycrystalline TiN thin films, where multilayer desorption is seen to occur above 200 K.<sup>11</sup> The activation energy for this process is estimated to be 14 kcal/mol by assuming that desorption follows a first-order rate law with a preexponential factor of 1 × 10<sup>13</sup> s<sup>−1</sup> and that the half-life of this process at 225 K is ~1 s (i.e., that the reaction goes to completion during the several seconds required to flash the sample to this temperature).<sup>22</sup>

The results of temperature-programmed desorption (TPD) experiments are in good agreement with the spectral observations discussed above. These studies reveal that a Cu(111) surface dosed with 1 L of Cu(hfac)<sub>2</sub> at 100 K loses a small amount of precursor to the gas phase at temperatures below ~240 K (Figure 2a, heating rate = 2 K/s). The resulting monolayer decomposes at elevated temperatures (see below). The origins of the two peaks in this figure are unclear at this time since the intensities of *both* features increase with increasing gas dose. We cannot rule out the possibility that the peak at ca. 170 K may be due to trace hfacH impurities which are significantly more volatile than Cu(hfac)<sub>2</sub> (see Figure 2b). Analysis of the larger, higher temperature peak places an *upper limit* of ~15 kcal/mol on the activation energy for desorption of Cu(hfac)<sub>2</sub> from a Cu(111) surface.

We have carried out analogous studies with hfacH. Exposure of a Cu(100) single crystal to 20 L of hfacH at 125 K leads to the formation of a multilayer of intact hfacH molecules on the surface (Figure 3, top trace). The RAIR spectrum contains several bands in the 1100–1400 cm<sup>−1</sup> region due to, inter alia, C–F and

(15) Lin, W.; Nuzzo, R. G.; Girolami, G. S., submitted for publication.

(16) Chai, K. M.; Shin, H.-K.; Hampden-Smith, M. J.; Kodas, T. T.; Duesler, E. N. *Inorg. Chem.* **1991**, *30*, 4293.

(17) Nakamoto, K.; Morimoto, Y.; Martell, A. E. *J. Phys. Chem.* **1962**, *66*, 346.

(18) Morris, M. L.; Moshier, R. W.; Sievers, R. E. *Inorg. Chem.* **1963**, *2*, 411.

(19) Dubois, L. H.; Zegarski, B. R. *J. Electrochem. Soc.* **1992**, *139*, 3295.

(20) Nakamoto, K.; Martell, A. E. *J. Chem. Phys.* **1960**, *32*, 588. Mikami, M.; Nakagawa, I.; Shimanouchi, T. *Spectrochim. Acta* **1967**, *23A*, 1037.

(21) Shimanouchi, T. *J. Phys. Chem. Ref. Data* **1977**, *6*, 993.

(22) Bent, B. E.; Nuzzo, R. G.; Zegarski, B. R.; Dubois, L. H. *J. Am. Chem. Soc.* **1991**, *113*, 1137.

**Table II.** Observed Vibrational Frequencies and Mode Assignments for Cu(hfac)(vtms) and vtms<sup>a</sup>

Cu(hfac)(vtms)/ Cu(100), 125 K <sup>b,c</sup>	neat Cu(hfac)(vtms) <sup>c,d</sup>	vtms/ Cu(111) <sup>e</sup>	vtms/ Cu(100) <sup>f</sup>	0.5 Torr vtms <sup>g</sup>	assignment <sup>h</sup>
	3045		3049	3193	2 × C=C stretch
	3020		3010	3061	CH <sub>2</sub> asym stretch
3030	2960		2958	3020	CH stretch
2956	2902	2895	2896	2968	CH <sub>3</sub> asym stretch
2922, 2900				2908	CH <sub>3</sub> sym stretch
2852				2860	overtone/combination of CH <sub>3</sub> deformations
			2798	2813	
(1634) <sup>i</sup>	(1608) <sup>i</sup>		1596	1600	C=C stretch
			1443	1445	CH <sub>3</sub> asym deformation
	1413	1405	1399	1409	CH <sub>2</sub> scissors
1258	1260	1225	1252	1256	CH <sub>3</sub> sym deformation
	970, 955	985	1008, 951	1011, 955	CH <sub>2</sub> twists wag
	845	830		849	CH <sub>3</sub> rock
	673, 588	660, 580		688	SiC stretch
	529			513	CH bend
		220			SiC rock

<sup>a</sup> All frequencies in cm<sup>-1</sup>. <sup>b</sup> IR, Figure 4. <sup>c</sup> Only those modes assignable to vtms are listed. Assignments of bands due to the hfac ligand are listed in Table I. <sup>d</sup> Reference 19. <sup>e</sup> EELS, Figure 5a. <sup>f</sup> IR, Figure 5b. <sup>g</sup> References 12 and 19. <sup>h</sup> Reference 25. <sup>i</sup> May also be due to the C=O stretch of the hfac ligand, see Table I.

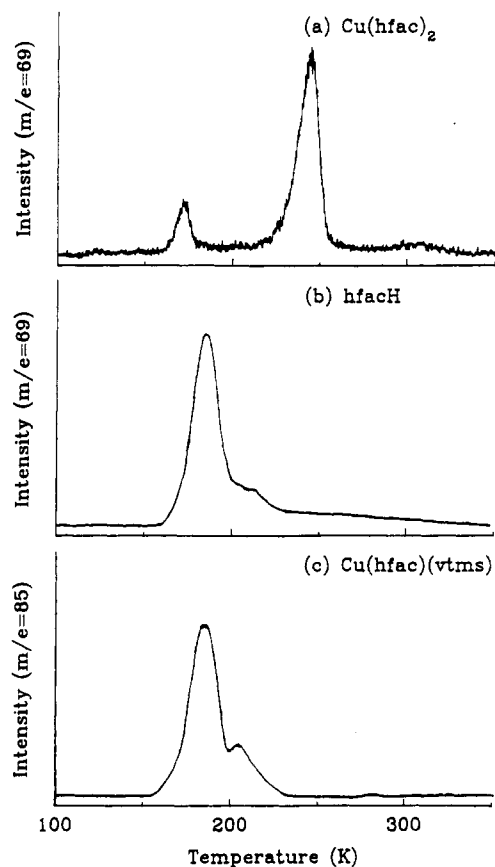


**Figure 2.** Temperature-programmed desorption spectra of (a) Cu(hfac)<sub>2</sub>, (b) hfacH, and (c) Cu(hfac)(vtms) adsorbed on a Cu(111) surface at ~100 K. The traces in a and b are for *m/e* = 69 (CF<sub>3</sub>), and those in c are for *m/e* = 85 (Me<sub>2</sub>SiCHCH<sub>2</sub>). The heating rate was 2 K/s.

C–C single bond stretching modes. The two modes at 1699 (C=O) and 1634 cm<sup>-1</sup> (C=C) suggest that the hfacH ligands exist exclusively as the enol tautomer,<sup>23</sup> since the diketone tautomer would show an additional peak at ~1800 cm<sup>-1</sup>.<sup>24</sup> Consistent with this, we observe a broad band extending from ~3550 to 2800 cm<sup>-1</sup> characteristic of hydrogen-bonded OH groups.<sup>23</sup>

Between 125 and 150 K the intensities of all of the peaks in Figure 3 decrease by a factor of ~5, which indicates that hfacH

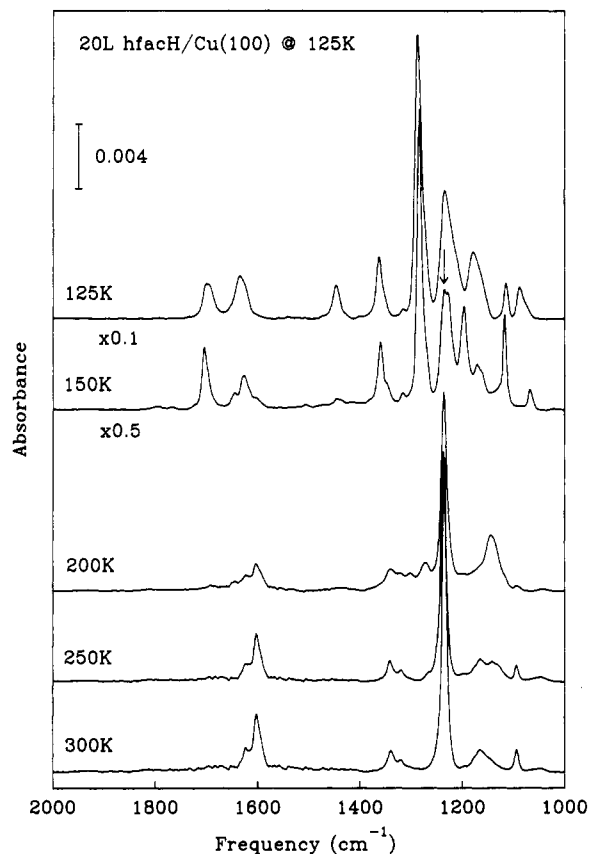


**Figure 3.** Infrared spectrum of a Cu(100) surface exposed to 20 L of hfacH at 125 K (upper trace). The adsorbate is in the enolate form. The physisorbed multilayer desorbs above ~150 K, leaving the surface covered with a monolayer of hfac ligands (see text). All spectra were recorded at 125 K.

is desorbing from the multilayer. Between 150 and 200 K the peaks due to physisorbed hfacH diminish further and are replaced with bands that are similar to those seen upon warming a Cu(100) surface dosed with Cu(hfac)<sub>2</sub> to 225 K (Figure 1, bottom trace). In order to generate this same species on the surface, the hfacH molecule must deprotonate to give surface-bound hfac groups and atomic hydrogen. This process must begin at low temperatures, since even at 150 K we observe a peak at 1235 cm<sup>-1</sup> characteristic of deprotonated hfac ligands (see arrow in Figure 3).

The RAIR spectrum of a Cu(100) surface dosed with 60 L of Cu(hfac)(vtms) at 125 K (Figure 4) reveals the presence of vtms as well as hfac. The presence of vtms is shown by the new peaks

(23) Tayyari, S. F.; Zeegers-Huyskens, Th.; Wood, J. L. *Spectrochim. Acta* 1979, 35A, 1265.

(24) Shigorin, D. N.; Sheverdina, N. I. *Dokl. Akad. Nauk. SSSR* 1954, 96, 561.

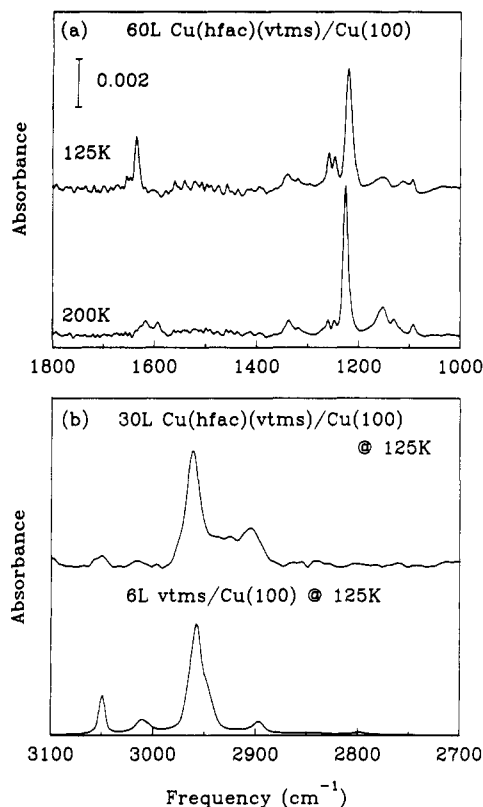


**Figure 4.** Infrared spectrum of a Cu(100) surface exposed to 60 L of Cu(hfac)(vtms) at 125 K (a, upper trace). Bands characteristic of both the hfac and vtms portions of the molecule are observed.<sup>19</sup> Mode assignments are summarized in Tables I and II. Warming the substrate to 200 K (lower trace) causes the vtms ligand to desorb, leaving the surface covered with a perpendicular-bonded hfac species (see text). All spectra were recorded at 125 K. In b the vibrational spectra in the CH stretching region for 20 L of Cu(hfac)(vtms) (upper trace) and 6 L of vtms (lower trace) physisorbed on Cu(100) at 125 K are compared.

at 1257 and 1246  $\text{cm}^{-1}$  ( $\text{CH}_3$  deformations, Figure 4a) and 2956, 2922, and 2852  $\text{cm}^{-1}$  (C–H stretching vibrations, Figure 4b, see also ref 25 and Table II). Care must be taken when dosing the surface at low temperatures, since trace vtms impurities are far more volatile than pure Cu(hfac)(vtms) and can easily block surface sites from further precursor adsorption (see Experimental Section). When the crystal is warmed to 200 K, the peaks assigned to vtms decrease in intensity; those attributed to the hfac ligand do not change. This is a clear indication that vtms is desorbing from the surface, and this conclusion is confirmed by TPD studies carried out on both Cu(100)<sup>19</sup> and Cu(111) substrates (see below). After vtms desorption is complete, the resulting infrared spectrum is similar to that of adsorbed Cu(hfac)<sub>2</sub> or hfacH at comparable temperatures (ref 12 and Figures 1 and 3, bottom traces). This lack of change in the spectrum of the hfac ligand upon warming implies that the copper–vtms bond in Cu(hfac)(vtms) is cleaved at low temperatures.

These observations are consistent with high-resolution electron energy loss (EELS) spectroscopy and temperature-programmed desorption experiments performed on Cu(111). If the surface is dosed with 1 L of pure vtms at 100 K, the molecule adsorbs intact, yielding a vibrational spectrum similar to that of the gas-phase species (Figure 5, upper trace and Table II). For comparison, the infrared spectrum of 6 L of vtms adsorbed on a clean Cu(100) surface at 125 K is shown in the lower trace of Figure 5. Upon ramping the crystal temperature, vtms desorbs intact to give one principal TPD feature centered at  $\sim 190$  K with a small shoulder sometimes appearing at  $\sim 220$  K.<sup>19</sup> These temperatures are very similar to the temperatures at which vtms desorbs from a Cu(111)

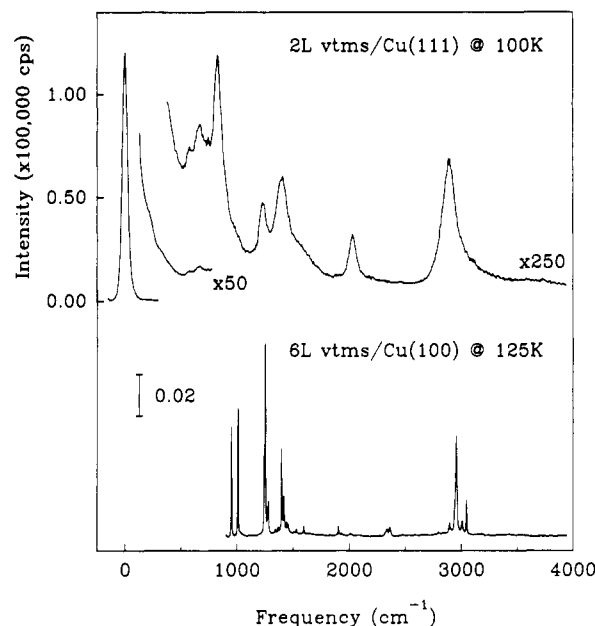


**Figure 5.** High-resolution EELS spectrum of a Cu(111) surface exposed to 2 L of vtms at 100 K (upper trace). The weak feature near 2050  $\text{cm}^{-1}$  is due to trace amounts of coadsorbed CO. For comparison, the infrared spectrum of 6 L of vtms adsorbed on Cu(100) at 125 K is shown in the lower trace. Both spectra are similar to that of gas-phase vtms.<sup>12,19,25</sup> Mode assignments are summarized in Table II.

surface dosed with Cu(hfac)(vtms) at 100 K (Figure 2c). Analysis of the TPD data according to the protocol of Redhead<sup>26</sup> (assuming a preexponential factor of  $1 \times 10^{13} \text{ s}^{-1}$ ) yields a value of 13–14 kcal/mol for the activation energy for the desorption of vtms from either Cu(111) or Cu(100).<sup>19</sup>

Infrared and mass spectrometry studies of Cu(hfac)(vtms) decomposition in the gas phase also show the copper–vtms bond to be weak. We have demonstrated previously that the infrared spectrum of Cu(hfac)(vtms) is merely the sum of the spectra of vtms and Cu(hfac)<sub>2</sub> with no significant shift in either the frequency or the intensity of any of the modes.<sup>12,19</sup> Furthermore, the Cu–vtms bond can be cleaved readily by heating the precursor to  $\sim 500$  K in the gas phase.<sup>12,27</sup> Studies of molecular compounds also show that copper is weakly coordinated to unsaturated hydrocarbons.<sup>16,28,29</sup> For example, <sup>1</sup>H NMR studies reveal that coordinated alkynes can be exchanged rapidly in solution, even at 180 K.<sup>16</sup> In addition, Cu(hfac)(diphenylacetylene) has a short C≡C distance (similar to that of free alkynes), a large C–C–Ph bond angle, and long Cu–C bond distances.<sup>16</sup> A recent low-temperature X-ray diffraction study of Cu(hfac)(vtms) yielded a similar structure.<sup>30</sup>

**Surface Reactions at 300 K.** High-resolution EELS spectra of a Cu(111) surface exposed to saturation doses of Cu(hfac)<sub>2</sub>, Cu(hfac)(vtms), and hfacH at 300 K are shown in Figure 6a, b, and c, respectively. The corresponding infrared spectra on a Cu(100) substrate have been published previously.<sup>12</sup> The spectra all contain strong peaks due to the hfac ligand and are very similar to the RAIR spectra obtained upon dosing a Cu(100) surface with any of these molecules at low temperature and heating to 200–250 K (Figures 1, 3, and 4). In spectrum a, the hfac ligands have migrated away from the central copper atom, since the three peaks near 1200  $\text{cm}^{-1}$  characteristic of pure Cu(hfac)<sub>2</sub> have disappeared. Similarly, spectrum b shows that no intact Cu(hfac)(vtms)

(26) Redhead, P. A. *Vacuum* **1962**, *12*, 203.

(27) Chiang, C.-M.; Dubois, L. H. *Mat. Res. Soc. Sym. Proc.*, in press.

(28) Chi, K. M.; Shin, H.-K.; Hampden-Smith, M. J.; Duesler, E. N.; Kodas, T. T. *Polyhedron* **1991**, *10*, 2293. Kumar, R.; Fronczek, F. R.; Maverick, A. W.; Lai, W. G.; Griffin, G. L. *Chem. Mater.* **1992**, *4*, 577.

(29) Reynolds, S. K.; Smart, C. J.; Baran, E. F.; Baum, T. H.; Larson, C. E.; Brock, P. J. *Appl. Phys. Lett.* **1991**, *59*, 2332.

(30) Norman, J. A. T.; Muratore, B. A.; Dyer, P. N.; Roberts, D. A.; Hochberg, A. K.; Dubois, L. H. *Proc. Int. Conf. Electron. Mat.* **1992**, (Eur. Mat. Res. Soc.), in press.

(25) Durig, J. R.; Natter, W. J.; Johnson-Streusand, M. *Appl. Spectrosc.* **1980**, *34*, 60.

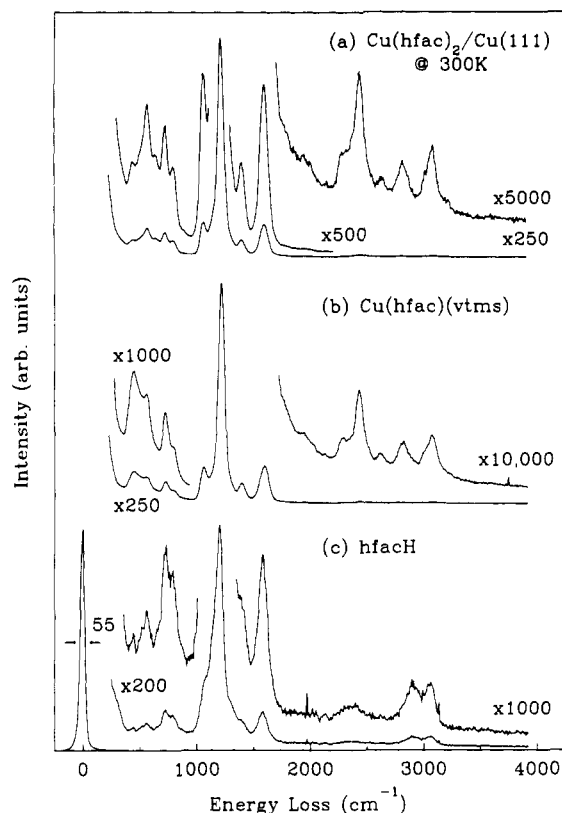


**Figure 6.** High-resolution EELS spectra of a Cu(111) surface exposed to saturation doses of (a) Cu(hfac)<sub>2</sub>, (b) Cu(hfac)(vtms), and (c) hfacH at 300 K. Similar vibrational spectra are observed for these three adsorbates on Cu(100) (see Figures 1, 3, and 4 and ref 12). Mode assignments are summarized in Table I. All spectra were recorded at 100 K.

molecules are present because, for example, the bands at 845 (CH<sub>3</sub> rock), 1260 (CH<sub>3</sub> sym deformation), and 2960 cm<sup>-1</sup> (CH stretch) characteristic of vtms are absent. The vtms ligands clearly dissociate from the Cu(hfac) centers and desorb from the surface very rapidly at 300 K, consistent with the low-temperature IR and TPD data. Both a and b are similar to the spectrum obtained by saturating a Cu(111) surface at 300 K with the free ligand hexafluoroacetylacetone, except that the weak overtone/combination bands at 2300–2800 cm<sup>-1</sup> are now even less intense (Figure 6c). The presence on the surface of H atoms from the deprotonation of hfacH is implied, but this fact has not yet been established directly.

Both infrared spectroscopy and high-resolution EELS show that the same surface species is formed at 300 K upon adsorption of Cu(hfac)(vtms), Cu(hfac)<sub>2</sub>, and hfacH.<sup>31</sup> It is also evident that the hfac groups have not undergone any fragmentation reactions at this temperature, as shown by the presence of the characteristic hfac C=O stretching mode at ~1610 cm<sup>-1</sup>. This has been confirmed by X-ray photoelectron spectroscopy for the adsorption of Cu(hfac)<sub>2</sub> and Cu(hfac)(1,5-cyclooctadiene) on evaporated silver films<sup>32</sup> and for Cu(hfac)<sub>2</sub> and Cu(hfac)(vtms) on a polycrystalline TiN substrate.<sup>11</sup> There are two important questions to consider: (1) How are the hfac groups oriented with respect to the surface? and (2) Are the hfac groups bound to terrace atoms, or are they present as adsorbed Cu(hfac) fragments?

The approximate orientation of the hfac groups with respect to the surface can be deduced by a comparison of the relative RAIR intensities with those of an isotropic sample of a hfac-

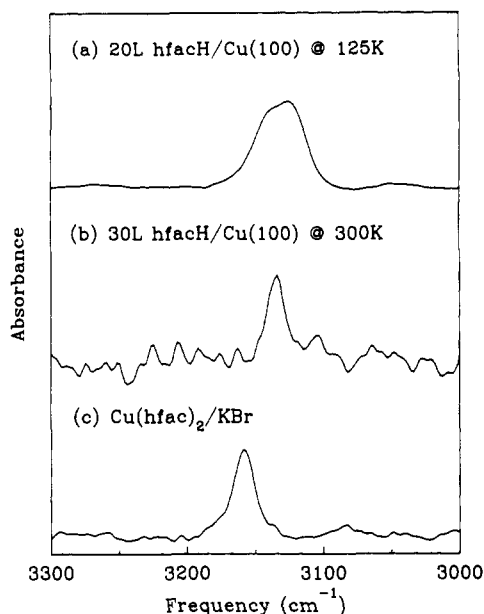
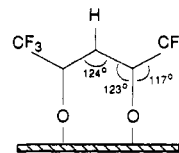


**Figure 7.** Infrared spectrum of 20 L of hfacH physisorbed on Cu(100) at 125 K (upper trace). If the Cu(100) surface is exposed to 30 L of hfacH at 300 K, then only a weak (0.00006 absorbance unit) C—H stretching vibration characteristic of the methyne hydrogen is observed (middle trace). For comparison, the infrared spectrum of Cu(hfac)<sub>2</sub> in a KBr pellet is shown at the bottom. The spectra have been normalized to a uniform peak height.

containing molecule. Since only those modes whose motions are perpendicular to the surface will be observed, an understanding of the normal modes of vibration of the adsorbate will allow us to determine its orientation.<sup>33</sup> The vibrational modes of the hfac ligand can be classified according to whether their motion is either in or out of the C(CO)CH(CO)C plane. In-plane motions include the C—H, C=O, C=C, and symmetric CF<sub>3</sub> stretches by analogy with the normal coordinate vibrational analysis of Cu(acac)<sub>2</sub>.<sup>20</sup> The antisymmetric CF<sub>3</sub> stretch and CF<sub>3</sub> rock have out-of-plane components. In many cases it is difficult to assign the observed bands to specific local vibrations of the adsorbate since most of these modes are of mixed character. Nevertheless, if we compare the intensities of the bands due to the surface-bound hfac ligands with those of a representative *planar* hfac-containing molecule (Cu(hfac)<sub>2</sub>), we conclude that the hfac ligand must be standing essentially perpendicular to the copper substrate. We base this conclusion on the observation of two diagnostic modes for the surface-bound hfac ligands: the C=O stretch at ca. 1620 cm<sup>-1</sup> and the C—H stretch at 3136 cm<sup>-1</sup>. If the geometries of the hfac ligands derived from the crystal structure of copper  $\beta$ -diketonates<sup>16,30,34</sup> are representative of the structures of the adsorbed species, then these two modes should be observed only if the plane of the hfac ligands is perpendicular to the surface.



The observation of the C=O stretch for the adsorbed hfac ligands is clearly shown by the data in Figures 1 and 3 (see also Figure 1 of ref 12). The weak C—H stretch from the dissociative chemisorption of hfacH on Cu(100) at 300 K is shown in the middle trace of Figure 7. The high frequency of this band is characteristic of the methyne hydrogen.<sup>20</sup> The vibrational spectrum of a multilayer of hfacH (upper trace) and that of bulk

(31) A single species with a vibrational spectrum similar to that observed here is seen from the adsorption of either Cu(hfac)<sub>2</sub> or Cu(hfac)(1,5-cyclooctadiene) on an evaporated silver film.<sup>32</sup> It appears that two different types of adsorbed species may be formed on *clean* TiN surfaces, however.<sup>11</sup>

(32) Cohen, S. L.; Liehr, M.; Kasi, S. *Appl. Phys. Lett.* **1992**, *60*, 50. *J. Vac. Sci. Technol.* **1992**, *A10*, 863.

(33) Ibach, H.; Mills, D. L. *Electron Energy Loss Spectroscopy and Surface Vibrations*; Academic: New York, 1982.

(34) Shin, H.-K.; Hampden-Smith, M. J.; Duesler, E. N.; Kodas, T. T. *Polyhedron* **1991**, *10*, 645.

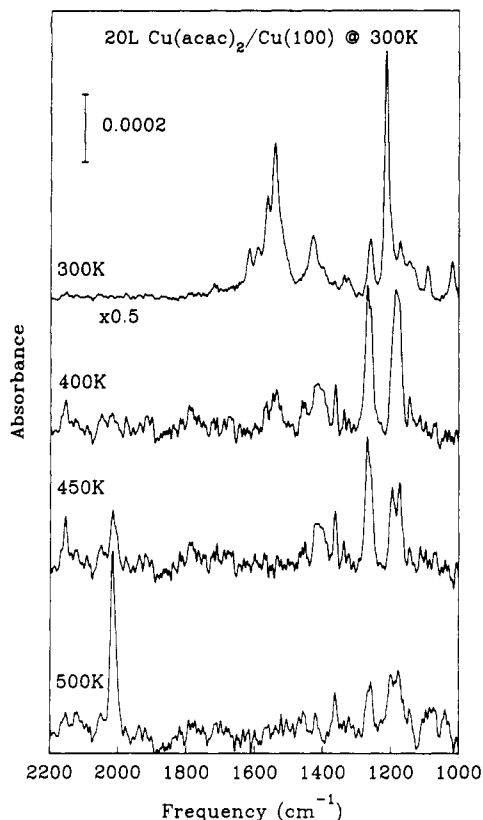


**Figure 8.** Infrared spectrum of a Cu(100) surface exposed to 20 L of Cu(acac)<sub>2</sub> at 300 K (upper trace). Detailed analysis of this spectrum indicates that the acac ligand is oriented perpendicular to the surface (see text). As with the data in Figure 11 for adsorbed hfac ligands, the spectra change dramatically as the surface is flashed to the indicated temperatures. All spectra were recorded at 300 K.

Cu(hfac)<sub>2</sub> (lower trace) are shown for comparison. Consistent with this proposed geometry, we observe some intensity for the C=C stretch ( $\sim 1650\text{ cm}^{-1}$ ). This band as well as the C=O and C—H stretches would be absent if the adsorbed hfac ligands were oriented parallel to the surface.

The assignment of the geometry of the hfac ligands is complicated by the fact that many of its in-plane modes will be parallel to the surface irrespective of the geometry of the adsorbate. Further, although the most intense band in the spectrum is a C—F stretching vibration ( $\sim 1235\text{ cm}^{-1}$ ), this band cannot be used to determine the orientation of the hfac ligands since its character is unknown (the frequency is intermediate between the symmetric and antisymmetric CF<sub>3</sub> stretches in bulk Cu(hfac)<sub>2</sub>, see Table I). Finally, we note that slight distortions from a rigorous perpendicular geometry or a small number of hfac ligands in different orientations at steps and/or defects cannot be ruled out in our experiments.

Further confirmation of the orientation of the  $\beta$ -diketonate ligand is provided by the infrared spectrum of adsorbed Cu(acac)<sub>2</sub>. A typical spectrum of the Cu(100) surface exposed to 20 L of Cu(acac)<sub>2</sub> at 300 K is shown in the upper trace of Figure 8. The adsorption of acacH yields a similar vibrational spectrum, which implies that both the Cu—acac and the acac—H bonds of the adsorbate are cleaved at this temperature. This observation is consistent with the studies of adsorbed Cu(hfac)<sub>2</sub>, Cu(hfac)(vtms), and hfacH discussed above. The perpendicular orientation of the resulting acac ligand is confirmed by the presence in the IR spectrum of the methyne C—H stretch ( $3092\text{ cm}^{-1}$ ), the C=O stretch ( $1563\text{ cm}^{-1}$ ), the degenerate in-plane CH<sub>3</sub> deformation ( $1430\text{ cm}^{-1}$ ), and the CH<sub>3</sub> rock ( $1024\text{ cm}^{-1}$ ); the dipole derivatives of all of these modes are parallel to the C—H axis.<sup>20</sup> The corresponding vibrations in Cu(acac)<sub>2</sub> are found at 3072, 1554, 1415, and  $1020\text{ cm}^{-1}$ , respectively.<sup>20</sup>

A similar conclusion about the structure of the adsorbed species is reached from an analysis of the high-resolution EELS data in

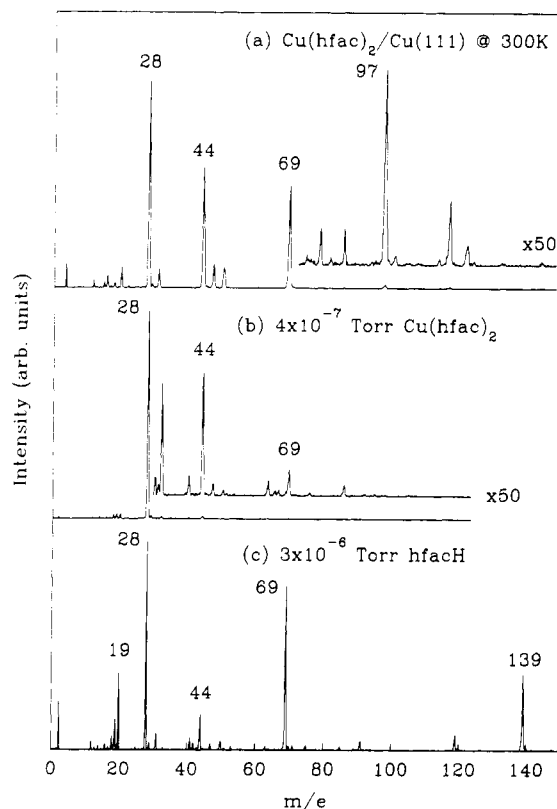


**Figure 9.** (a) IDMS spectrum of the species desorbing from a Cu(111) surface exposed to 20 L of Cu(hfac)<sub>2</sub> at 300 K. Data were obtained between 350 and 650 K at a heating rate of 2 K/s. Similar spectra have been recorded for Cu(hfac)(vtms) and hfacH.<sup>12</sup> Mass spectra of gas-phase Cu(hfac)<sub>2</sub> and hfacH recorded with the same quadrupole settings are shown in traces b and c, respectively.

Figure 6, although the selection rule is not rigorous in this case. The analysis is complicated by impact scattering,<sup>33</sup> which can account for the relatively intense C—H stretching and overtone/combination bands. Since similar vibrational spectra are observed irrespective of whether Cu(hfac)<sub>2</sub>, Cu(hfac)(vtms), or hfacH is adsorbed, we conclude that the adsorbate *cannot* be bonded as a Cu(hfac) species. There may be some interaction with copper adatoms, however, since recent XPS studies of Cu(hfac)<sub>2</sub> and Cu(hfac)(1,5-cyclooctadiene) adsorbed on evaporated silver films show copper to be in an oxidation state midway between 0 and +1.<sup>32</sup> Further, the observation of a  $\pi^* \leftarrow \pi$  transition in the O 1s XPS spectra of Cu(hfac)<sub>2</sub> and Cu(hfac)(vtms) adsorbed on TiN show that the delocalized  $\pi$  system of the hfac ligands remains intact on this substrate.<sup>11</sup>

**Ligand Decomposition at Elevated Temperatures.** Since Cu(hfac)(vtms), Cu(hfac)<sub>2</sub>, and hfacH yield the same surface-bound hfac groups at 300 K, it is not surprising that the subsequent reaction chemistry and the spectra at higher temperatures are virtually identical.

Figure 9a shows an integrated desorption mass (IDMS) spectrum<sup>35</sup> taken during the decomposition of a saturation monolayer of Cu(hfac)<sub>2</sub> on Cu(111) at temperatures between 350 and 650 K. The spectrum contains peaks at  $m/e = 19$  (F), 28 (CO), 31 (CF), 44 (CO<sub>2</sub>), 47 (COF), 50 (CF<sub>2</sub>), 69 (CF<sub>3</sub>),<sup>36</sup> 97 (COCF<sub>3</sub>), and 117 (HOCFCF<sub>3</sub>). The desorbing species is not molecular Cu(hfac)<sub>2</sub> (nor does it contain any copper) since the peaks characteristic of atomic copper at  $m/e = 63$  and 65 are absent. Similarly, the desorbing species is not hfacH because peaks at  $m/e = 139$  (parent—CF<sub>3</sub>) and 119 (parent—CF<sub>3</sub>—HF) characteristic of hfacH (Figure 6b) are also not seen. Mass spectral studies

(35) Dubois, L. H. *Rev. Sci. Instrum.* **1989**, *60*, 410.

(36) Based on the results of recent isotopic labeling studies, we conclude that desorption at  $m/e = 69$  at low temperatures may be due in part to C<sub>3</sub>O<sub>2</sub>H(D). Lin, W.; Nuzzo, R. G.; Girolami, G. S., unpublished observations.

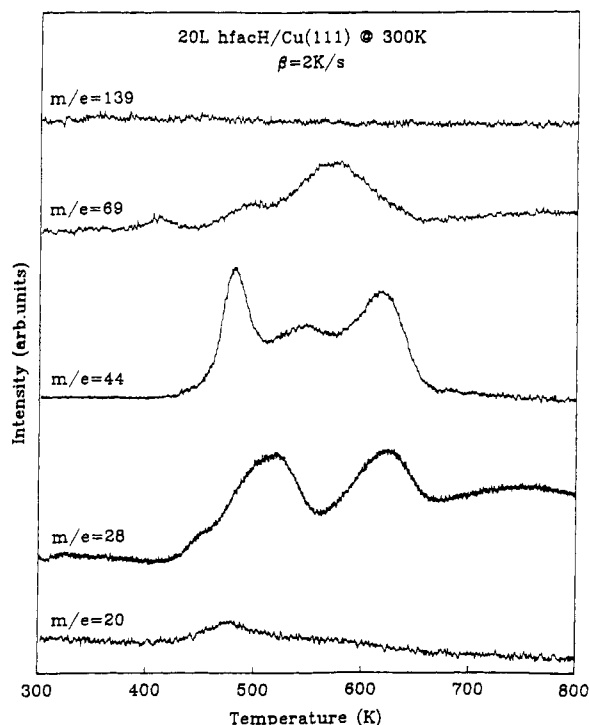


**Figure 10.** TPD spectra recorded after exposing a clean Cu(111) surface to 20 L of hfacH at 300 K. Traces for  $m/e = 139$  (hfacH- $\text{CF}_3$ ), 69 ( $\text{CF}_3$ ), 44 ( $\text{CO}_2$ ), 28 ( $\text{CO}$ ), and 20 (HF) are shown. Peak intensities between spectra are arbitrary. A similar series of data was observed from the adsorption of  $\text{Cu}(\text{hfac})_2$ .<sup>12</sup> The origins of the different peaks are discussed in the text.

of hfacH decomposition on Cu(111) between 350 and 650 K yield comparable results. Further, IDMS studies of  $\text{Cu}(\text{hfac})(\text{vtms})$  adsorption on Cu(111) at 300 K show no evidence of vtms desorption at elevated temperatures (peaks at  $m/e = 85$  (parent- $\text{CH}_3$ ) and 59 ( $\text{Si}(\text{CH}_3)_2\text{H}$ )). We conclude, therefore, that the desorbing species must be the result of fragmentation of the adsorbed hfac ligands.

Kinetic information can be obtained from temperature-programmed desorption experiments. Representative traces for the decomposition of hfacH on Cu(111) (20-L dose at 300 K) are shown in Figure 10. Similar spectra were observed for  $\text{Cu}(\text{hfac})_2$ <sup>12</sup> and  $\text{Cu}(\text{hfac})(\text{vtms})$ . The  $m/e = 69$  ( $\text{CF}_3$ ) channel shows that desorption of fluorocarbons occurs as a single, broad feature at temperatures between 500 and 650 K. On the basis of the cracking pattern measured here (Figure 9,  $I_{69}(\text{CF}_3):I_{50}(\text{CF}_2):I_{31}(\text{CF}) = 1.00:0.20:0.19$ ) and elsewhere,<sup>11</sup> this peak *cannot* be assigned to the desorption of  $\text{CF}_3$  radicals ( $I_{69}(\text{CF}_3):I_{50}(\text{CF}_2):I_{31}(\text{CF}) = 0.47:1.00:0.88$ <sup>37</sup>). This species has been assigned previously to the desorption of  $\text{CF}_4$ , although the observed cracking pattern is also consistent with a  $\text{CF}_3\text{CO}$  group or a larger molecule that contains this fragment. This species can further dissociate in the electron impact ionizer to yield a cracking pattern similar to that observed in Figure 9 (see, for example, the mass spectrum of  $\text{CF}_3\text{COCF}_3$  in ref 38).

In contrast to the single peak observed for fluorocarbon desorption, three features are seen in both the  $m/e = 28$  ( $\text{CO}$ ) and the  $m/e = 44$  ( $\text{CO}_2$ ) channels between 425 and 650 K. This indicates that some of the gas-phase CO and  $\text{CO}_2$  products are derived from the decomposition of the same surface intermediates. In addition, a broad desorption peak is seen for CO from 650 to 775 K. The  $m/e = 28$  and 44 peaks do not result from adsorbed CO or  $\text{CO}_2$  since these species are only weakly bound to copper

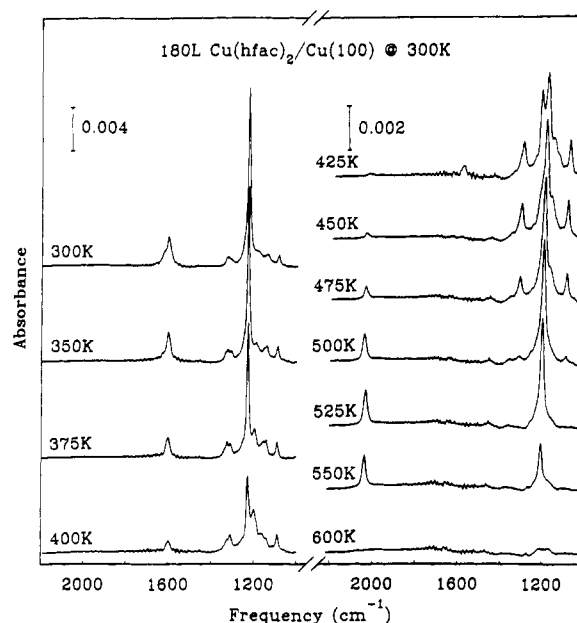


**Figure 11.** Reflection-absorption infrared spectra of a Cu(100) surface exposed to 180 L of  $\text{Cu}(\text{hfac})_2$  at 300 K. The vibrational spectra change dramatically as the sample is flashed to the indicated temperatures. The origin of some of the new modes is discussed in the text. All spectra were recorded at 300 K.

surfaces (binding energy  $\sim 7$  kcal/mol for  $\text{CO}_2$ <sup>39</sup> and  $< 14$  kcal/mol for  $\text{CO}$ <sup>40</sup>) so desorption would be complete by 180 K. Furthermore, the CO is not derived from the cracking of  $\text{CO}_2$  in the mass spectrometer ionizer because the relative intensity of the CO peak in this spectrum is  $\sim 20$  times too large as determined by IDMS (Figure 9a).<sup>38</sup> The absolute cross sections for the ionization of these two molecules are also quite similar.<sup>41</sup> The onset of a small amount of fluorine desorption at  $m/e = 19$  at 420 K is coincident with the low-temperature features observed in the  $m/e = 28$  and 44 traces. Therefore, the TPD data clearly show that adsorbed hfac ligands decompose in a stepwise fashion at temperatures between 400 and 775 K to liberate fluorine, CO,  $\text{CO}_2$ , and fluorinated hydrocarbons.

In order to obtain more direct information about the identity of the species present on the copper surface above 300 K, infrared spectra were collected after heating a Cu(100) single crystal dosed at 300 K with 180 L of  $\text{Cu}(\text{hfac})_2$  (Figure 11). The initial spectrum recorded at 300 K shows peaks at 1607 ( $\text{C}=\text{O}$  stretch), 1332 ( $\text{CF}_3$  stretch), 1238 ( $\text{CF}_3$  stretch), and 1147 and 1093  $\text{cm}^{-1}$  ( $\text{C}-\text{H}$  bends) characteristic of an intact hfac group. As the temperature increases, all of these peaks disappear and several new features grow in. The new peak at 1205  $\text{cm}^{-1}$ , which first appears at 375 K, reaches a maximum intensity at 475 K and then diminishes. Based on the 30- $\text{cm}^{-1}$  shift to lower frequency, we assign this peak to the symmetric C-F stretch of a surface-bound  $\text{CF}_3$  ligand. Using the dipole selection rule, we conclude that the adsorbate is oriented approximately perpendicular to the surface. This conclusion is consistent with the orientation of  $\text{CH}_3$  fragments on Pt(111).<sup>42</sup> Our assignment is further substantiated by the temperature dependence of this peak, which shows that the intensity of the 1205- $\text{cm}^{-1}$  band decreases over the same temperature range (475–600 K) in which  $m/e = 69$  is seen to desorb in the TPD data (Figure 10).

A second, new peak is observed at 2038  $\text{cm}^{-1}$  that first appears at 425 K and continues to increase in intensity up to 525 K. Since

(37) Freund, R. S., unpublished observations.

(38) Heller, S. R.; Milne, G. W. A. *EPA/NIH Mass Spectral Data Base*; Washington, DC, Vol. 1.

(39) Rasmussen, P. B.; Taylor, P. A.; Chorkendorff, I. *Surf. Sci.* **1992**, 269/270, 352. Taylor, P. A.; Rasmussen, P. B.; Chorkendorff, I. *J. Vac. Sci. Technol.* **1992**, A10, 2570.

(40) See, for example: Hinch, B. J.; Dubois, L. H. *J. Electron. Spectrosc. Relat. Phenom.* **1990**, 54/55, 759.

(41) Freund, R. S.; Wetzel, R. C.; Shul, R. *Phys. Rev. A* **1990**, 41, 5861.

(42) Zaera, F.; Hoffmann, H.; Griffiths, P. R. *J. Electron. Spectrosc. Relat. Phenom.* **1990**, 54/55, 705.



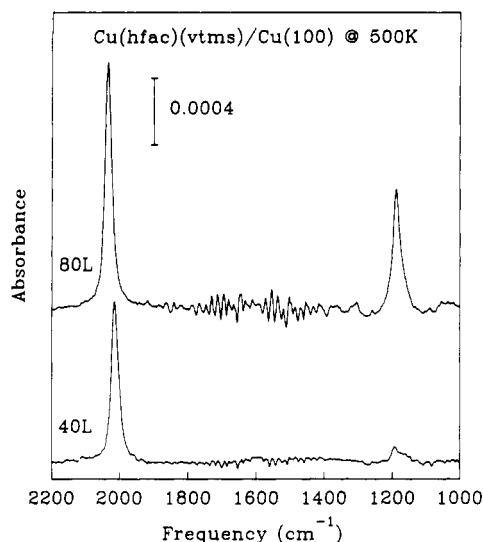


**Figure 12.** Infrared spectra of a Cu(100) surface exposed to 40 (lower trace) and 80 L (upper trace) of Cu(hfac)(vtms) at 500 K. These data clearly show that the two peaks at 2030 and 1220  $\text{cm}^{-1}$  are not correlated. Both spectra were recorded at 500 K.

the temperature dependence of the intensity of this mode is different from that of the peak at 1205  $\text{cm}^{-1}$ , it must be due to a different species. This species can be formed independently by dosing a Cu(100) crystal with 40 L of Cu(hfac)(vtms) at 500 K and collecting the spectrum at this temperature (Figure 12). Although the frequency of this peak is consistent with the presence of weakly chemisorbed CO, this species is not stable on copper surfaces above  $\sim 180$  K,<sup>40</sup> and thus this possibility can be ruled out. CO adsorption on oxidized copper sites is also quite weak<sup>43</sup> and cannot account for the observed peak. Furthermore, the species responsible for the 2038- $\text{cm}^{-1}$  band cannot contain fluorine, since this peak is still formed in analogous experiments with the *unfluorinated* molecules Cu(acac)<sub>2</sub> and acacH (Figure 8, bottom trace). Finally, we can rule out the possibility that this band is due to a surface acetylide or acetylene complex since the C $\equiv$ C stretch for such species should occur at much lower frequencies<sup>44</sup> and no corresponding C-H stretch is observed.

We tentatively assign this band to the C $\equiv$ O stretch of an adsorbed ketenylidene ( $\text{C}\equiv\text{C}=\text{O}$ ) fragment. The IR frequency is very similar to those observed in ketenylidene metal cluster compounds such as  $[\text{Os}_3(\text{CO})_9(\mu^3\text{-CCO})]_2$ —which has CO stretches at 2031, 1994, 1956, and 1899  $\text{cm}^{-1}$ <sup>45</sup>—and  $[\text{Ru}_3(\text{CO})_6(\mu\text{-CO})_3(\mu^3\text{-CCO})]_2$ —which has terminal CO stretches at 2023, 1982, 1952, and 1899  $\text{cm}^{-1}$ .<sup>46</sup> The assignment of a specific band to the ketenylidene ligand in these clusters has not been reported; however, the 2038- $\text{cm}^{-1}$  band observed in the RAIR spectra is in the correct frequency range. We tentatively assign a weak feature near 900  $\text{cm}^{-1}$  in the high-resolution EELS spectrum recorded on a Cu(111) surface to the C-C stretch of this species. A similar peak is found near  $\sim 920$   $\text{cm}^{-1}$  in the infrared spectrum on Cu(100). Again, the CF<sub>3</sub> and ketenylidene intermediates must be associated with terrace atoms since they are observed from the decomposition of Cu(hfac)<sub>2</sub> and Cu(hfac)(vtms) as well as hfacH. In addition, small amounts of ketenylidene species are seen from the decomposition of adsorbed acacH.

It has been shown that ketenylidene ligands in metal cluster compounds can lose carbon monoxide upon heating to form metal carbide clusters.<sup>45,47,48</sup> If the behavior of surface-bound kete-

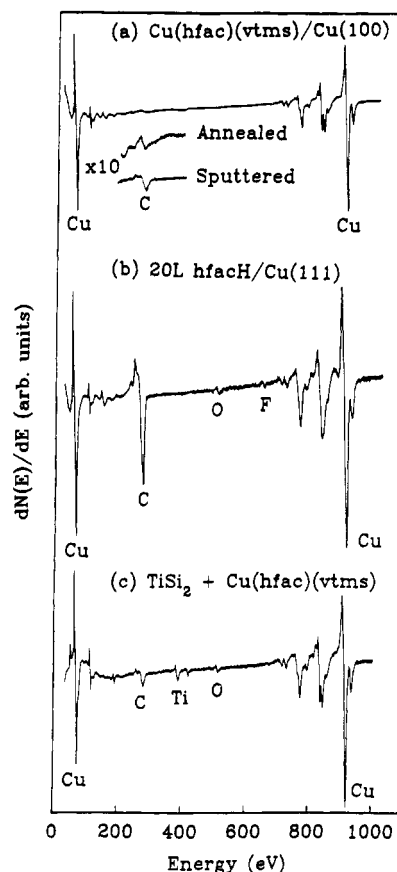


**Figure 13.** Auger electron spectrum of (a) a clean Cu(100) surface exposed to 20 L of Cu(hfac)(vtms) at 300 K and flashed to 600 K. Only trace carbon impurities are observed. In the lower trace the experiments were repeated, except the surface was sputtered with  $\sim 5$   $\mu\text{A}$  of 1 keV  $\text{Ne}^+$  ions at room temperature for 5 min *without* annealing to create a significant number of surface defects. In this latter case, slightly more carbon is observed. In b the Cu(111) surface was exposed to 10 cycles of 20 L of hfacH at 300 K and then heated to 650 K. Significantly more carbon is seen in this case. Trace c shows that a thin film of relatively pure copper can be grown from Cu(hfac)(vtms) under high vacuum conditions ( $1 \times 10^{-5}$  Torr, 500 K, 10 min) on a  $\text{TiSi}_2$  substrate.

nylidene groups is similar, then further heating of this group should lead to desorption of CO and formation of surface-bound carbon atoms; this is precisely what is seen when the surface is heated to above  $\sim 600$  K. Thus we believe that the TPD feature at ca. 620 K in the  $m/e = 28$  (CO) channel (Figure 10) is due to decarbonylation of the ketenylidene groups. The presence of surface carbon after this process is completed is shown by the persistence of a small signal at  $\sim 270$  eV in the Auger spectrum, Figure 13a. Oxygen and fluorine are not detected. We note, however, that halogens are extremely sensitive to electron-stimulated desorption.<sup>49</sup> Attempts to remove the ketenylidene species by reaction with either water or  $\text{H}_2$  at 350 K under UHV conditions ( $\sim 100$ -L gas exposures) proved unsuccessful.

Copper adatoms and/or surface defects play a minimal role in the decomposition reaction of the surface hfac species since the same process is observed for Cu(hfac)<sub>2</sub>, Cu(hfac)(vtms), and hfacH. Analyses of the corresponding data for Cu(acac)<sub>2</sub> and acacH adsorption on Cu(100) lead to the same conclusion. The role of defects is shown more explicitly in Figure 13a, where a Cu(100) surface is sputtered at room temperature without further annealing and then exposed to 20 L of Cu(hfac)(vtms) at 300 K, followed by flashing to 600 K. The resulting Auger spectrum

(43) Davydov, A. A.; Budneva, A. A. *React. Kinet. Catal. Lett.* **1984**, *25*, 121.

(44) Crowell, J. E.; Bent, B. E.; Koel, B. E.; Mate, C. M.; Somorjai, G. A. *In press*.

(45) Sailor, M. J.; Shriver, D. F. *Organometallics* **1985**, *4*, 1476.

(46) Went, M. J.; Sailor, M. J.; Bogdan, P. L.; Brock, C. P.; Shriver, D. F. *J. Am. Chem. Soc.* **1987**, *109*, 6023.

(47) Hriljac, J. A.; Swebston, P. N.; Shriver, D. F. *Organometallics* **1985**, *4*, 158.

(48) Kolis, J. W.; Holt, E. M.; Shriver, D. F. *J. Am. Chem. Soc.* **1983**, *105*, 7307.

(49) See, for example: Westphal, D.; Goldmann, A. *Surf. Sci.* **1983**, *131*, 92, 113.

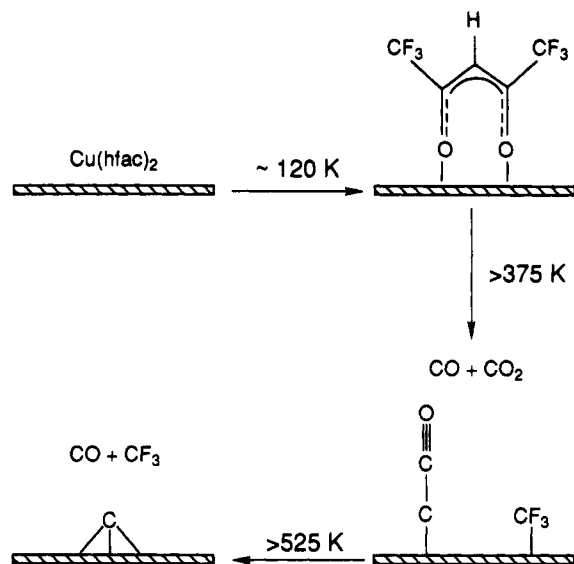


**Figure 14.** Schematic representation of the reaction of a copper  $\beta$ -diketonate complex with a copper surface. The presence of a perpendicularly bonded hfac species and  $\text{CF}_3$  and ketenylidene fragments are confirmed by infrared spectroscopy. Under UHV conditions, copper adatoms do not appear to be involved in the decomposition process since a similar reaction scheme is seen for adsorbed hfacH and acacH.

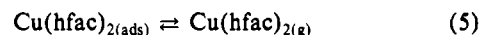
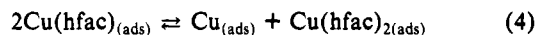
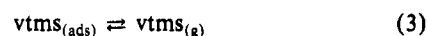
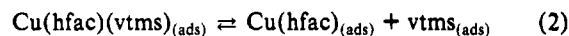
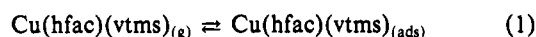
shows little increase in surface carbon. A significant concentration of carbon can be built up on the surface by repeated cycles of precursor adsorption at room temperature followed by flashing to 700 K (see Figure 13b). In this case, small amounts of both oxygen and fluorine are also observed. Two other potential sources of carbon include the cracking of the hfac ligand to yield  $\text{CO}_2$  and the decomposition of the  $\text{CF}_3$  fragments to give  $\text{CF}_4$ .

Interestingly, under certain conditions a clean copper film can be grown in *high* vacuum. If a titanium disilicide thin film (prepared as discussed elsewhere<sup>50</sup>) is exposed to  $1 \times 10^{-5}$  Torr of  $\text{Cu}(\text{hfac})(\text{vtms})$  for 10 min at 500 K, a thin copper film can be grown. The Auger spectrum of this material is shown in Figure 13c. The film is relatively clean, with only trace amounts of carbon and oxygen observed.<sup>51</sup> We cannot rule out the presence of these species by adsorption from the background and/or cracking of residual gases in the electron gun of the Auger analyzer since the pressure in the vacuum system while these spectra were recorded was in the  $10^{-7}$  Torr range. Consistent with this notion, the shape of the carbon peak at  $\sim 270\text{ eV}$  is characteristic of a graphitic (as opposed to a carbide) species.

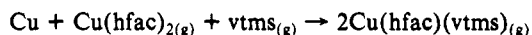
**Surface Reaction Mechanism.** The overall mechanism for the reaction of copper  $\beta$ -diketonate complexes with copper surfaces under ultra-high-vacuum conditions is shown in Figure 14. Above 200 K, the ligands migrate from the adsorbed precursor to give hfac groups on the surface. These species are oriented approximately parallel to the substrate. The surface-bound hfac ligands remain unchanged until  $\sim 375\text{ K}$ , when they begin to fragment to yield CO and  $\text{CO}_2$  (which promptly desorb) and trifluoromethyl and ketenylidene species (which remain on the surface). At much higher temperatures ( $\sim 525\text{ K}$ ) the trifluoromethyl groups begin to desorb. Finally, the ketenylidene groups decarbonylate above 550 K and leave behind a carbon residue. This decarbonylation reaction accounts for one source of carbon found in copper films grown from  $\text{Cu}(\text{hfac})_2$  in the absence of hydrogen.

Although a surface disproportionation reaction clearly takes place during film growth from copper(I)  $\beta$ -diketonates at elevated pressures,<sup>5,6</sup> the details of the mechanism are still unknown. The present studies shed some light on this process. One possible reaction scheme is summarized below. We note that the process

appears to be identical on Cu(111) and Cu(100).



Here (ads) refers to an adsorbed species. Step 1 appears to be unactivated since  $\text{Cu}(\text{hfac})(\text{vtms})$  readily adsorbs on a clean copper substrate at low temperatures. From our TPD and temperature-dependent IR studies, we conclude that step 2 has an activation energy of  $\lesssim 14\text{ kcal/mol}$ . This is also a reversible process, as Norman et al. have shown that



is rapid at 410 K.<sup>6</sup> Steps 3 and 5 are also facile, occurring with activation energies on the order of 14–15 kcal/mol. From our studies, it is clear that decomposition of the hfac ligands is a higher energy process and is suppressed at elevated pressures. This leaves the surface disproportionation reaction (step 4) to be, we believe, rate limiting. While this process is known to occur in solution at room temperature,<sup>52</sup> the effects of constraining both reactants to 2 dimensions *may* increase the activation energy for this process dramatically. This conclusion is supported by recent measurements of the activation energy for film growth from  $\text{Cu}(\text{hfac})(\text{trimethylphosphine})$ ,  $\text{Cu}(\text{hfac})(2\text{-butyne})$ , and  $\text{Cu}(\text{hfac})(1,5\text{-cyclooctadiene})$ , where, although the Cu–ligand bond strengths vary significantly,<sup>19</sup> the activation energies are all quite similar (21–26 kcal/mol).<sup>53</sup> Steps 1 through 5 (above) may be too simplistic, however, as more recent pressure-dependent studies of copper film growth from  $\text{Cu}(\text{hfac})(\text{vtms})$  have shown.<sup>54</sup>

One important aspect of the deposition of copper films remains to be addressed: If both  $\text{Cu}(\text{hfac})_2$  and  $\text{Cu}(\text{hfac})(\text{vtms})$  yield hfac ligands on the surface (which subsequently fragment in a similar manner), then why can clean copper films be grown from  $\text{Cu}(\text{hfac})(\text{vtms})$  in the absence of a carrier gas? The explanation of this apparently contradictory behavior must be related to the coverage of the adsorbate on the surface under the deposition conditions. As discussed above, thin film growth from Cu(I)  $\beta$ -diketonates proceeds via a surface disproportionation reaction, but this is inherently a bimolecular process. Under UHV conditions, however, bimolecular reactions are never favored over unimolecular decomposition reactions, even if the activation energies for the latter processes are significantly higher: the surface coverage is generally too low for the bimolecular process to occur.<sup>22</sup> As the pressure is raised above  $\sim 10^{-5}$  Torr the surface concentration of hfac ligands increases, the disproportionation reaction becomes facile, and clean copper films can be grown (Figure 13c).

### 3. Conclusions

Although reactions conducted under UHV conditions do not always follow the same pathways as those occurring at elevated pressures, these experiments can provide useful insight into film growth under more “real” CVD conditions. From the studies presented here, we have demonstrated the ability to (a) observe intermediates on the surface during the ligand decomposition process, (b) measure activation energies for the cleavage of metal–ligand bonds, and (c) provide a mechanism for carbon incorporation into the growing film. In addition, we provide evidence for the rate-limiting step in the disproportionation of copper(I)  $\beta$ -diketonates at elevated pressures. Complementary studies on the adsorption of  $\text{Cu}(\text{hfac})(\text{vtms})$  on  $\text{TiN}^{11}$  and  $\text{SiO}_2^{19,30}$  substrates have provided information on the nucleation process as well as on the limits to selective growth. We believe that with care in the interpretation of data such as these, the kind of in-

(50) Dubois, L. H.; Zegarski, B. R.; Girolami, G. S. *J. Electrochem. Soc.* **1992**, *139*, 3603.

(51) A similar conclusion has been reached recently using platinum substrates: Parmeter, J., private communication.

(52) Jacq, J.; Cavalier, B.; Bloch, O. *Electrochim. Acta* **1968**, *13*, 1119.

(53) Jain, A.; Chi, K.-M.; Shin, H.-K.; Farkas, J.; Kodas, T. T.; Hampden-Smith, M. J. *Semicon. Int.* In press.

(54) Jain, A.; Kodas, T. T., private communication.

formation provided by single crystal/UHV studies can be used to improve the design and processing of CVD precursors.

#### 4. Experimental Section

High-resolution EELS, TPD, and IDMS experiments were performed in a diffusion- and titanium-sublimation-pumped ultra-high-vacuum chamber with a base pressure near  $1 \times 10^{-10}$  Torr. The system was equipped with four-grid low-energy electron diffraction (LEED) optics (Varian), a single-pass cylindrical mirror analyzer (PHI) for Auger electron spectroscopy (AES), a differentially pumped quadrupole mass spectrometer (Vacuum Generators), and a high-resolution electron energy loss spectrometer (McAllister Technical Services). For the EELS experiments, the angle of the incident electron beam ( $60^\circ$  to the surface normal) and its energy (4–5 eV) were held constant and electrons were collected only in the specular direction. The elastic scattering peak from an adsorbate-covered surface had an intensity of  $>10^5$  cps and a full width at half maximum of 6–8 meV ( $50\text{--}60\text{ cm}^{-1}$ ). For the TPD and IDMS experiments the heating rate was 2 K/s.

Infrared experiments were conducted in a second small UHV chamber also equipped for Auger electron spectroscopy and low-energy electron diffraction. The system was interfaced to a conventional Fourier transform infrared spectrometer (Mattson Instruments) using reflection optics ( $\sim f/15$ ). The angle of incidence was  $85^\circ$  and only the reflected, p-polarized light was collected using a liquid nitrogen cooled, narrow band MCT detector. Typically 2048 scans were averaged at  $4\text{-cm}^{-1}$  resolution. In the variable temperature experiments, the sample was raised to the indicated temperature for  $\sim 2$  s and then cooled to the dosing temperature before data collection was initiated.

The 1–1.3-cm diameter Cu(111) and Cu(100) single crystal disks ( $>99.999\%$ , Monocrystals) were oriented, cut, and polished using standard techniques. The samples were mounted on small, temperature-controlled molybdenum blocks which could be heated to  $\sim 1200$  K by a tungsten filament or cooled to  $\sim 100$  K via copper braids attached

to a liquid nitrogen reservoir. Temperatures were measured using a chromel–alumel thermocouple inserted into the copper substrate. The crystals were cleaned of trace carbon, sulfur, and oxygen impurities by repeating cycles of neon ion sputtering ( $1000\text{ eV}$ ,  $8\text{--}10\text{ }\mu\text{A}/\text{cm}^2$ ) at both 300 and 970 K followed by annealing in vacuum at 970 K. Sample cleanliness and order were carefully monitored by AES and LEED, respectively. Samples were sputtered and annealed before each adsorption experiment.

Anhydrous Cu(hfac)<sub>2</sub> and hfacH (99%) were purchased from Strem. Cu(hfac)(vtms) was obtained from Schumacher. Cu(acac)<sub>2</sub> (97%), acacH (99+%), and vtms (97%) were purchased from Aldrich. All adsorbates were thoroughly degassed by repeated freeze–pump–thaw cycles prior to introduction into the vacuum chambers. Care was taken to completely dehydrate the Cu(hfac)<sub>2</sub> (dark purple crystals) by heating under vacuum prior to dosing. Gas dosing of the more volatile species was performed by backfilling the UHV systems while the lower vapor pressure materials were introduced into the chambers through a heated, effusive molecular beam doser. Further, the headgas from the Cu(hfac)(vtms) source was continuously pumped during dosing in order to minimize vtms contamination in the effluent. Gas exposures were not corrected for the varying sensitivities of the different ionization gauges.

**Acknowledgment.** We thank R. S. Freund (AT&T Bell Laboratories), J. Parmeter (Sandia National Laboratories), and A. Jain and T. T. Kodas (University of New Mexico) for communicating results prior to publication. We also thank B. R. Zegarski for help in collecting some of the infrared data. G.S.G. acknowledges support from the Department of Energy under contract DEFG02-91ER45439 and is the recipient of a Camille and Henry Dreyfus Teacher-Scholar Award and an A. P. Sloan Foundation Research Award. P.M.J. acknowledges the receipt of a University of Illinois Department of Chemistry Fellowship.

## Interannular Proton Transfer in Thermal Arenium Ions from the Gas-Phase Alkylation of 1,2-Diphenylethane

Fulvio Cacace,<sup>\*,†</sup> Maria Elisa Crestoni,<sup>†</sup> Simonetta Fornarini,<sup>†</sup> and Dietmar Kuck<sup>‡</sup>

*Contribution from the Dipartimento di Studi di Chimica e Tecnologia delle Sostanze Biologicamente Attive, Università "La Sapienza" I-00185, Roma, Italy, and Fakultät für Chemie der Universität Bielefeld, D-4800 Bielefeld 1, Germany. Received July 27, 1992*

**Abstract:** The first demonstration of *thermal* interannular proton shifts in gaseous bicyclic arenium ions and the evaluation of their Arrhenius parameters have been achieved with the radiolytic technique. The model ions have been obtained by alkylation of  $\text{C}_6\text{D}_5\text{CH}_2\text{CH}_2\text{C}_6\text{H}_5$  with radiolytically formed  $\text{Me}_3\text{C}^+$  ions in isobutane at sufficiently high pressure (630–1730 Torr) to ensure that the processes of interest obey thermal kinetics. From the extent of interannular H/D scrambling in the alkylated products, measured as a function of the arenium ions' lifetime, the rate constant for the  $\text{H}^+(\text{D}^+)$  ring-to-ring transfer in the para-substituted arenium ions has been estimated to be  $(1.3 \pm 0.4) \times 10^7$  ( $(2.9 \pm 0.6) \times 10^6$ )  $\text{s}^{-1}$  at  $47^\circ\text{C}$ . A temperature-dependence study covering the range from 47 to  $150^\circ\text{C}$  has allowed the evaluation of the Arrhenius parameters for the interannular  $\text{H}^+(\text{D}^+)$  transfer, giving  $E_a = 6.3 \pm 0.2$  ( $8.0 \pm 0.2$ )  $\text{kcal mol}^{-1}$  and  $\log A = 11.4 \pm 0.4$  ( $11.9 \pm 0.3$ ). Further mechanistic insight into the detailed mechanism of gas-phase alkylation is provided by other kinetic results. In particular, the significant interannular H/D discrimination of  $\text{Me}_3\text{C}^+$ , which favors the unlabeled ring of  $\text{C}_6\text{D}_5\text{CH}_2\text{CH}_2\text{C}_6\text{H}_5$  by a factor of 1.7 at  $47^\circ\text{C}$ , provides further evidence for the reversible character of aromatic *tert*-butylation suggested by previous radiolytic and mass spectrometric studies on monocyclic arenes. The higher *tert*-butylation rate (2.9:1 at  $120^\circ\text{C}$ ) of 1,2-diphenylethane than of toluene supports recent mass spectrometric results pointing to the formation of stable complexes between  $\text{Me}_3\text{C}^+$  and  $\alpha,\omega$ -diphenylalkanes.

Proton shifts in aromatic systems have been the subject of extensive studies by NMR techniques in acid solutions<sup>1</sup> and by computational methods.<sup>2</sup> Their occurrence in gaseous arenium ions is well documented by the results of chemical ionization (CI) and ion cyclotron resonance (ICR) mass spectrometric investi-

gations.<sup>3</sup> A kinetic study was recently reported of 1,2 proton shifts in gaseous arenium ions<sup>4</sup> based on the radiolytic technique,<sup>5</sup> which

<sup>†</sup> Università "La Sapienza".

<sup>‡</sup> Universität Bielefeld.

(1) (a) Brouwer, D. M.; Mackor, E. L.; MacLean, C. In *Carbonium Ions*; Olah, G. A., Schleyer, P. v. R., Eds.; Wiley: New York, 1984; Vol. II, p 837. (b) Kopytug, V. A. In *Contemporary Problems in Carbonium Ions Chemistry III*; Rees, Ch, Ed.; Springer-Verlag: Berlin, 1984; p 119 and references therein.